Journal of Carcinogenesis

Original Article

# Constitutive over expression of IL-1β, IL-6, NF-κB, and Stat3 is a potential cause of lung tumorgenesis in urethane (ethyl carbamate) induced Balb/c mice

Chandradeo Narayan, Arvind Kumar*

School of Biotechnology, Faculty of Science, Banaras Hindu University, Varanasi, Uttar Pradesh, India

E-mail: k_arvindk@rediffmail.com
*Corresponding author

Published: 24 July, 2012
Journal of Carcinogenesis 2012, 11:9
This article is available from: http://www.carcinogenesis.com/content/11/1/9


Received: 24 December, 2011
Accepted: 3 February, 2012

## Abstract

**Background:** Lung cancer is a leading cause of cancer death. There has been found a substantial gap in the understanding of lung cancer genesis at the molecular level. We developed urethane (ethyl carbamate) induced lung tumor mice model to understand the mechanism and molecules involved in the cancer genesis. There might be many molecules involved, but we subsequently emphasized here the study of alternation in the expression of NF-κB, Stat3, and inflammatory cytokines interleukin-1β and interleukin-6 to hypothesize that the microenvironment created by these molecules is promoting tumor formation. **Materials and Methods:** 7–8 week old Balb/c mice of either sex were given intraperitoneal (i.p.) injection of urethane (1g/kgbw) for eight consecutive weeks. Histopathological analysis was done to detect abnormality or invasions occurred in the lung tissues. Automated cell counter was used to count the number of inflammatory cells. The expression of NF-κB, Stat3, and IL-1β was observed at translational level by western blot, while the expression of IL-1β and IL-6 was observed at transcriptional level by semiquantitative reverse transcriptase polymerase chain reaction (RT-PCR) method. Secretion of IL-1β and IL-6 in the blood was measured by enzyme-linked immunosorbent assay (ELISA) method at different time intervals. **Results:** Histopathological analysis showed various lung cancer stages hyperplasia, atypical adenomatous hyperplasia, and adenocarcinoma. Increased population of inflammatory cells, persistant expression of NF-κB, Stat3, pStat3, and IL-1β at translational level, while at transcriptional level constitutive enhanced expression of IL-1β and IL-6 followed by increased secretion of IL-1β and IL-6 in the blood were observed in urethane-injected mice in comparison to phosphate buffer saline (PBS) injected mice at 12, 24, and 36 weeks. **Conclusions:** Overexpression of key molecules such as NF-κB, Stat3, pStat3, IL-1β, and IL-6 might have caused chronic inflammation, leading to the progression of lung cancer.

**Keywords:** Adenocarcinoma, NF-κB, proinflammatory cytokines, Stat3, urethane

Access this article online

Quick Response Code:

Website: www.carcinogenesis.com

DOI: 10.4103/1477-3163.98965

## BACKGROUND

Lung cancer has become one of the most common causes of cancer death in human.[1] Worldwide death toll due to lung cancer is approximately 1.2 million per year.[2] The number of lung cancer affected individuals throughout the world has been increased several times in recent years. Lung cancer is a highly complex neoplasm[3] consisting of two common histological types. The two types are small cell lung carcinoma (SCLC)

and nonsmall cell lung carcinoma (NSCLC). NSCLC are further classified as adenocarcinoma (AD), squamous cell carcinoma (SCC), and large cell neuroendocrine carcinoma.[4] Out of these types and subtypes, AD is a most common form of lung cancer.[5] Chronic inflammation is implicated in multistages of carcinogenesis to contribute tumor initiation and progression by several mechanisms including acceleration of cell cycle, cell proliferation and stimulation of tumor neo-vascularization.[6,7]

Urethane or ethyl carbamate (EC) is a chemical carcinogen present in tobacco leaves, tobacco smoke, [8] and in fermented food products, such as bread, yogurt, and cheese,[9] formed by the reaction of urea with alcohol [10, 11]. The concentration of EC (urethane) in some food and beverages[12-14] has been documented in the Table 1. Urethane specifically promotes the development of lung tumors from nonciliated airway epithelial (Clara) or type II alveolar epithelial cells in mice.[15,16] Balb/c mice are considered as an intermediate-susceptible for the development of lung tumor by urethane administration.[17] Urethane-induced lung AD has been well characterized and accepted as model for human lung AD.[18,19] The pathways connecting transcription factors (TFs) and cytokine-dependent inflammation and tumor formation in the lung induced by urethane have not been well deciphered so far.

## MATERIALS AND METHODS

### Chemicals

Urethane (Sigma chemical company, St Louis, MO), ethylenediamine tetraacetic acid (EDTA) (Merck, Mumbai, India), protease inhibitor cocktail (Thermo scientific, Rockford, USA), page ruler™ plus prestained protein ladder (Fermentas, USA); primary antibodies β-Actin (C4), (SC-47778); NF-κB p65 (C-20), (SC-372); Stat3 (C-20), (SC-482); pStat3 (Tyr705), (SC-7993); interleukin-1β (IL-1β), (I3767, Sigma); secondary antibodies goat anti-rabbit IgG HRP-conjugated, (SC-2030); donkey anti-goat IgG HRP-conjugated, (SC-2033); rabbit anti-mouse IgG HRP-conjugated, (HPO5,Genei, Bangalore); super signal west pico chemiluminescent substrate, 134078 (Pierce, Thermo Scientific, Rockford, USA). SC stands for Santa Cruz Biotechnology (CA, USA).

**Table 1: Concentration of urethane or ethyl carbamate in various foods and beverages**

| Reported by | Food and beverage | Concentration of ethyl carbamate |
|---|---|---|
| Hasnip *et al.* (2007) | Spirit drinks | 0.01-6.2 mg/L |
| | Whisky | <0.01 mg/L |
| | Beer | <0.01 mg/L |
| | Wine | 0.01–0.025 mg/L |
| | Sake | 0.08–0.17 mg/L |
| | Vinegar | 0.033 mg/L |
| | Cake | <0.01 mg/kg |
| | Bread | <0.01 mg/kg |
| | Sauerkeaut | 0.029 mg/kg |
| | Yeast extract | 0.041 mg/kg |
| | Cheese | <0.01 mg/kg |
| | Soybean paste | <0.01 mg/kg |
| | Soy sauce | 0.01-0.084 mg/kg |
| | Yogurt | <0.01 mg/kg |
| | Christmas pudding | 0.02 mg/kg |
| EFSA 2007 | Stone fruit brandy | 0.01-22 mg/L |
| Park *et al* 2007 | Fermented soy sauce | 0.01-0.1 mg/kg |

### Animals and experimental design

7–8 weeks old Balb/c mice of either sex, approximately having equal body weight were taken. Mice were distributed into two groups. Each group contains 8 mice numbered separately and one group was intraperitoneal (i.p.) injected with urethane dissolved in phosphate buffer saline (PBS), while another group was i.p. injected with PBS (control). All the mice were kept in hygienic condition at room temperature (RT) with a 12-h light/dark cycle, and provided with standard animal feed and water *ad libitum*. Tumors were induced by i.p. injection of urethane 1g/kgbw of mice for eight consecutive weeks and 6 to 8 month latency period. Mice were sacrificed for observation at 0, 12, 24, and 36 weeks from group of urethane-injected mice and PBS-injected mice. Body weight of each mouse was recorded weekly up to their sacrifice. Animal ethical rules were followed as per the guidelines given by the Animal Ethical Committee Institute of Medical Sciences (IMS), Banaras Hindu University (BHU), Varanasi, India.

### Histopathology

Lung's tissues were fixed over night in Bouin's solution followed by washing and dehydration in a graded series of ethanol. Finally, lung tissues samples were embedded in the paraffin. Paraffin-containing lung tissues were cut into the 5-$\mu$m-thick sections at the median transverse level. Sections were de-paraffinized using xylene and graded series of ethanol. Sections were mounted on glass slides, stained, and counterstained with hematoxylin and eosin (H&E), respectively, for microscopic examination.

### Peripheral blood cell counting

40 $\mu$l blood samples were collected from the retro-orbital sinus, by using a capillary pipette containing EDTA anticoagulant. The samples were used for complete blood cell count by automated Hematology analyzer KX-21 (Sysmex Corporation, Japan).

### SDS-PAGE and western blot

Lung tissues from urethane-injected mice and PBS-injected mice were used for protein extraction using lysis buffer. Lysis

buffer contains 50 mM Tris-Cl (pH-7.4), 150 mM NaCl, 0.5% Triton X-100, 5 mM EDTA (pH-8), and protease inhibitors cocktail. The concentration of each protein sample was estimated by Bradford assay, equalized and 50 $\mu$g/well was loaded on each lane of 10% SDS-PAGE for transcription factor TF and 12% sodium dodecyl sulphate-polyacrylamide gel electrophoresis SDS-PAGE for cytokines. Separated proteins were transferred to the polyvinylidene difluoride membranes (PVDF) at 20V/4$^0$C for overnight. The membranes were blocked with 5% nonfat dry milk in tris-buffer saline tween-20 TBST (1xTBS, 0.2% Tween 20) buffer at RT for 1 h. The membrane was washed thrice with TBST and incubated separately in the TBST buffer containing either primary antibody NF-κB p65, Stat3, pStat3 (Tyr705), IL-1β, or β-Actin separately, each having dilution of 1:1000. Separate PVDF membrane with protein samples were incubated with each primary antibody, thrice washed with TBST and then incubated separately into horse-radish peroxidase conjugated species-specific secondary antibody with a dilution of 1:5000 at RT for 1 h. After washing thrice with TBST to each PVDF membrane, the chemiluminascence substrate was poured all over membrane. The primary antibody specific proteins made visible by detecting chemifluorescence emission by exposing to the kodak X-ray film. To confirm equal protein loading, membranes were striped and reprobed with mouse monoclonal anti-β-actin primary antibody.

### Isolation of total RNA and semiquantitative PCR (RT-PCR)

Expression of IL-1β and IL-6 in lungs was studied by semiquatitative RT-PCR. For this, total RNA was isolated using Trizol (Invitrogen, Carlsbad, CA, USA) as per manufacturer's instructions. The tissue was homogenized in Trizol reagent and chloroform was added for phase separation. Colorless upper aqueous phase was gently taken out in separate tube and precipitated with isopropanol. Precipitated RNA was centrifuged at 10,000 rpm at 4°C. The pellet was retained to wash with 70% ethanol. Washed pellet was air dried and dissolved in diethyl pyrocarbonate (DEPC) -treated double distilled water. The concentration and purity of RNA was determined using nanodrop spectrophotometer (ND-1000, Wilmington, USA). First, strand of cDNA was synthesized by using AMV RT-PCR kit (105566, Banglore Genei, India) as follows: 1–5 $\mu$l (0.1–1 $\mu$g) total RNA, 1 $\mu$l Oligo $(dT)_{18}$, and RNAse free water to make total volume 10 $\mu$l. The vial containing sample solution was placed at 65°C for 10 min and at RT for 2 min. The sample was spun briefly and other components, e.g., RT enzyme, dNTP, RNase inhibitors, and RT buffer, were added. Sample solution was properly mixed, briefly centrifuged, and incubated at 42°C for 1 h, followed by incubation at 95°C for 2 min to stop the reaction. Finally, samples containing single cDNA strand were centrifuged for few seconds and kept on ice till PCR.

The amplification of IL-1β and IL-6 was done using MJ mini thermal cycler (Bio Rad, California, USA). The primers and amplicon sizes were as follows: IL-β forward primer 5'-GACCTTCCAGGATGAGGACA-3', reverse primer 5'-AGGCCACAGGTATTTTGTCG-3' with a product size 273bp; IL-6 forward primer 5'-TCTCCAGCAACGAGGAGAAT-3' reverse primer 5'-TGTGATCTGAAACCTGCTGC-3' with a product size 348bp; β-actin forward primer 5'-AGCCATGTACGTAGCCATCC-3' reverse primer 5'-CTCTCAGCTGTGGTGGTGAA-3' with a product size 227bp.

The parameters for the amplification of IL-1β and IL-6 were as follows: 94°C for 2 min, 94°C for 45 s, 52°C for 30 s, 72°C for 60 s for 35 cycles at 72°C for 2 min. The PCR products were separated on 2% agarose gel by electrophoresis along with DNA ladder of 100 bp. Gel was visualized under UV light in gel documentation system alpha imager EC (Alpha innotech, Japan).

### Enzyme-linked immunosorbent assay

IL-1β and IL-6 level in mice serum were measured by using highly specific quantitative sandwich Enzyme-linked immunosorbent assay (ELISA) kit (EMIL1B & EM2IL6 Pierce Biotechnology, Thermo scientific, Rockford, USA). ELISA was performed according to the manufacturer's instructions. 50 $\mu$l of biotinylated antibody reagent was added to each well of ELISA plate and then 50 $\mu$l test samples was added in duplicate to each well. Reagent in well were mixed and incubated for 2 h at RT, followed by three gentle washing with wash buffer. 100 $\mu$l of streptavidin-HRP solution was added to each well and incubated for 30 min at RT. 100 $\mu$l of TMB substrate solution was added, mixed by shaking and incubated 30 min for color development. Reaction was terminated by adding 100 $\mu$l of stop solution. Finally optical density was measured at 450 nm in chemiluminescent ELISA plate reader machine.

### Electrophoretic mobility shift assay

For the isolation of nuclear proteins, the pellet from minced lung tissues were resuspended in a modified RIPA lysis buffer containing 50 mM Tris, pH-7.4, 1% NP-40, 150 mM NaCl, 1 mM EDTA, 0.5% sodium deoxycholate, and protease inhibitor cocktail (Thermo scientific, Rockford, USA) with repeated vortexing on ice lysates were spun at 14,000 rpm for 25 min at 4°C to obtain supernatant designated as nuclear proteins. The concentration of proteins was determined by spectrophotometric method and the proteins were stored in aliquots at -80°C till further use. For binding reaction

and detection, light shift chemiluminescent Electrophoretic mobility shift assay (EMSA) and chemiluminescent nucleic acid detection module were used (Thermo scientific, Rockford, USA). Briefly, 100 fmol of labeled probe was incubated with nuclear extract (10$\mu$g proteins) in a total volume of 20 $\mu$l for 30 min at RT with binding buffer. To prevent nonspecific binding of nuclear proteins, 1$\mu$l of poly dI:dC was added. Protein-DNA complexes were separated from unbound DNA using 6% native PAGE. NF-κB and Stat3 binding oligonucleotide consensus sequence were as follows: NF-κB binding oligonucleotide consensus sequence biotin probe-5'- biotin -AGTTGAGGGGACTTTCCCAGGC-3', Stat3 binding oligonucleotide consensus sequence biotin probe- 5'-biotin-GATCCTTCTGGGAATTCCTAGATC-3'

### Statistical analysis

All the experiments were conducted three times and were reproducible. The bands were analyzed and quantitated using computer-assisted densitometry (Alpha innotech corporation, Japan). For RT-PCR and western blots, the band intensity was measured. Data were expressed as mean ± SEM; pair-wise comparisons were made by student's *t*-test. $P < 0.05$ were considered as significant.

## RESULTS

### Effect of urethane on body weight

The initially (at zero week) average body weight recorded for urethane-injected group and PBS-injected group were 20.75 and 17.88 g, respectively. Body weight of urethane-injected mice decreased up to fourth week (from 20.75 to 16.42 g), followed by continuous increase in the body weight up to 28 weeks (from 16.42 to 33.30 g). After 28 weeks, body weight of urethane-injected mice again decreases (from 33.30 to 30.05 g) but the body weight of PBS-injected mice increased continuously up to 36 weeks (from 17.88 to 34.05 g) [Figure 1].

### Effect of urethane on the lung organ index

Lung organ index of urethane-injected and PBS-injected mice were calculated at different time interval, i.e., at 0, 12, 24, and 36 week after sacrifice of mice. The lung organ index surprisingly increases 1.4, 1.6, and 1.72 folds at 12, 24, and 36 week, respectively, in the urethane-injected mice as compared to PBS-injected mice [Figure 2].

Organ index = weight of organ (g)/body of weight of mice (g) x 100

### Histopathological analysis of lung tissues section

The histopathological slide of urethane-injected lung tissues showed different adenoma stages [Figure 3]. Variable degree of atypia or hyperplasia shows abnormality with increase in the number of normal cells and its arrangement [Figure 3b]. Atypical adenomatous hyperplasia (AAH) shows severe cellular atypia with minimal septal inflammation and minimal septal fibrosis, cuboidal to low columnar in shape, sparse cytoplasm, inconspicuous nucleoli, distinct boundary

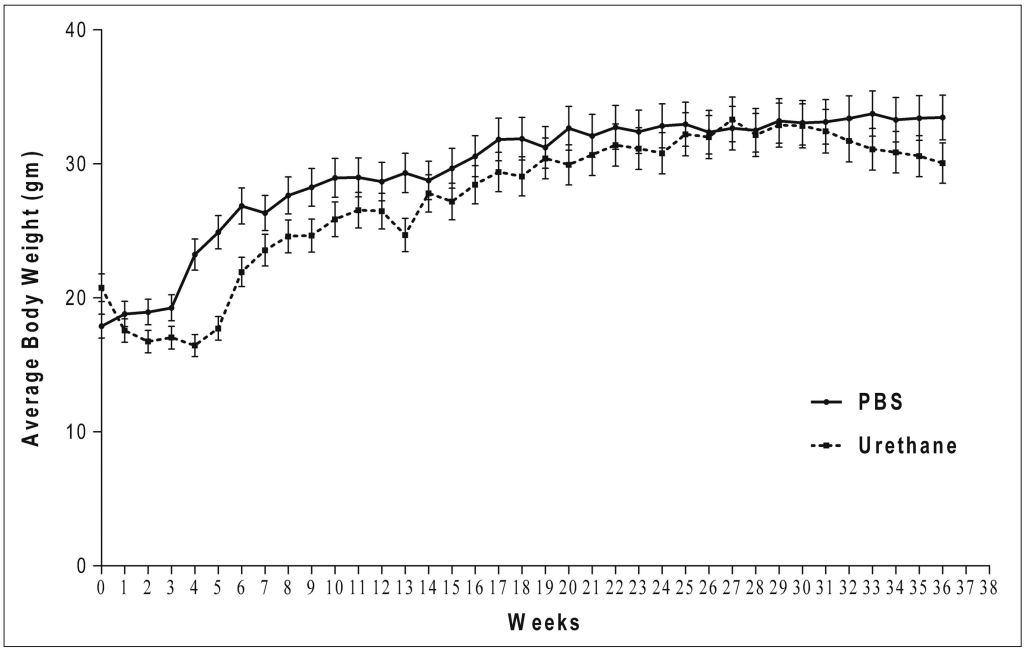


**Figure 1: Line graphs showing the average body weight (in grams) of urethane-injected and PBS- (phosphate buffer saline) injected control Balb/c mice. Body wt. was taken up to 36 weeks. (Data reported as the mean ± SEM for n = 8 per group and compared against PBS-injected mice.)**

with small lesions [Figure 3c]. AD shows the epithelial cells making up the tumor mass, severe septal inflammation and septal fibrosis, cuboidal to columnar in shape, moderate to abundant amount of eosinophilic cytoplasm, pleiomorphic nuclei are located centrally at base occasional prominent nucleolus or refractile pseudoinclussions, irregular boundary with severe lesions [Figure 3d].

## Quantitation of inflammatory cells in peripheral blood

Counting of total leukocytes, lymphocytes, monocytes, and neutrophils in peripheral blood samples of urethane-injected mice was done. The peripheral blood samples were collected at 0, 12, 24, and 36 week after urethane and PBS injection in mice [Figure 4]. The number of monocytes 2.92, 4.19, and 3.68 folds [Figure 4a], neutrophils 1.75, 2.21, and 2.09 folds [Figure 4b], lymphocytes 1.39, 1.71, and 2.26 folds [Figure 4c], and total leukocytes 1.41, 1.54, and 2.45 folds [Figure 4d] were higher in urethane-injected mice compared to PBS-injected mice at 12, 24, and 36 week, respectively.

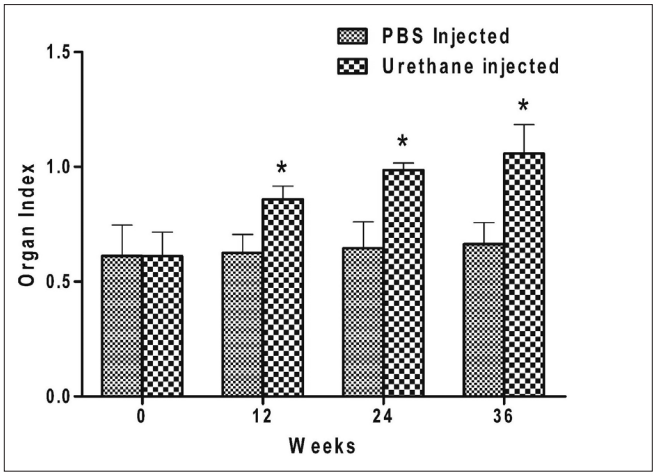


**Figure 2: Lung organ index of urethane-injected and PBS-injected controls Balb/c mice at 0, 12, 24, and 36 weeks (Data reported as the mean ± SEM for n = 8 per group and compared against PBS control by using a Student t-test. *P* < 0.05 were considered significant.)**

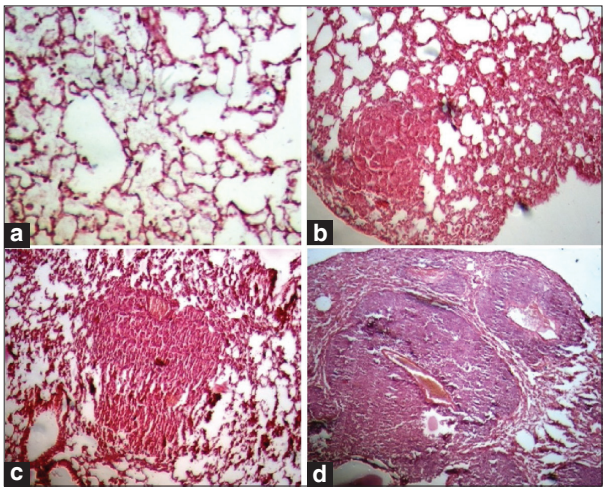


**Figure 3: Histopathological analysis of lung tissues of (a) PBS-injected control mice, (H and E, x50) (b) hyperplasia in urethane-injected lung tissues, (H and E, x50) (c) atypical adenomatous hyperplasia (AAH) in urethane-injected lung tissues, (H and E, x50) (d) adenocarcinoma in urethane-injected lung tissues (H and E, x50)**

## Translational expression of transcription factors and pro-inflammatory cytokines

Western blotting was performed to check the expression of TF pStat3, Stat3, NF-κB, and proinflammatory cytokines IL-1β at translational level in lung tissue of urethane-injected and PBS-injected mice at 0, 12, 24, and 36 week [Figure 5]. Immunoblots revealed almost equal expression of pStat3, Stat3, NF-κB, and IL-1β protein in the PBS-injected mice lung tissue samples at 0, 12, 24, and 36 week [Figure 5], while in urethane-injected mice lung tissue samples the expression level of pStat3, Stat3, NF-κB, and IL-1β proteins comparatively increased by 2.39, 2.36, 1.69, and 3.68 folds, respectively, at 12 week [Figure 5], 6.03, 5.48, 2.23, and 10 folds, respectively, at 24 week [Figure 5], and 3.01, 5.34, 2.44, and 9.77 folds, respectively, at 36 week [Figure 5] in comparison to PBS-injected mice lung tissue samples. The expression level of these proteins in urethane-injected and PBS-injected mice lung tissue samples at 0 week was almost equal.

## Gene expression of pro-inflammatory cytokines at transcription level

The effect of urethane on the expression of proinflammatory cytokines IL-1β and IL-6 at mRNA level was assessed in lung tissues of urethane-injected and PBS-injected mice at 0, 12, 24, and 36 week [Figure 6] by semiquantitative RT-PCR. The expression level of IL-1β and IL-6 was almost equal in PBS-injected mice lung tissue samples at 0, 12, 24, and 36 week [Figure 6], whereas in urethane-injected mice lung tissue samples showed upregulated expression of IL-1β and IL-6 by 5.6 and 4.5 folds, respectively, at 12 week, 9.4 and 2.8 folds, respectively, at 24 week [Figure 6], while 10 and 6.6 folds, respectively, at 36 week [Figure 5] compared to PBS-injected mice lung tissue samples. At zero week in urethane-injected mice lung tissues and PBS-injected mice tissues shows equal expression level of both IL-1β and IL-6.

## Production and secretion of pro-inflammatory cytokines

To determine the synthesis and secretion of pro-inflammatory cytokines (IL-1β and IL-6) level in blood, ELISA was performed with the serum samples isolated at 0, 12, 24, and 36 week [Figure 7] after urethane injection and PBS injection. IL-1β protein level was found elevated by 1.28, 1.72, and 2.26 folds at 12, 24 and 36 week, respectively, in

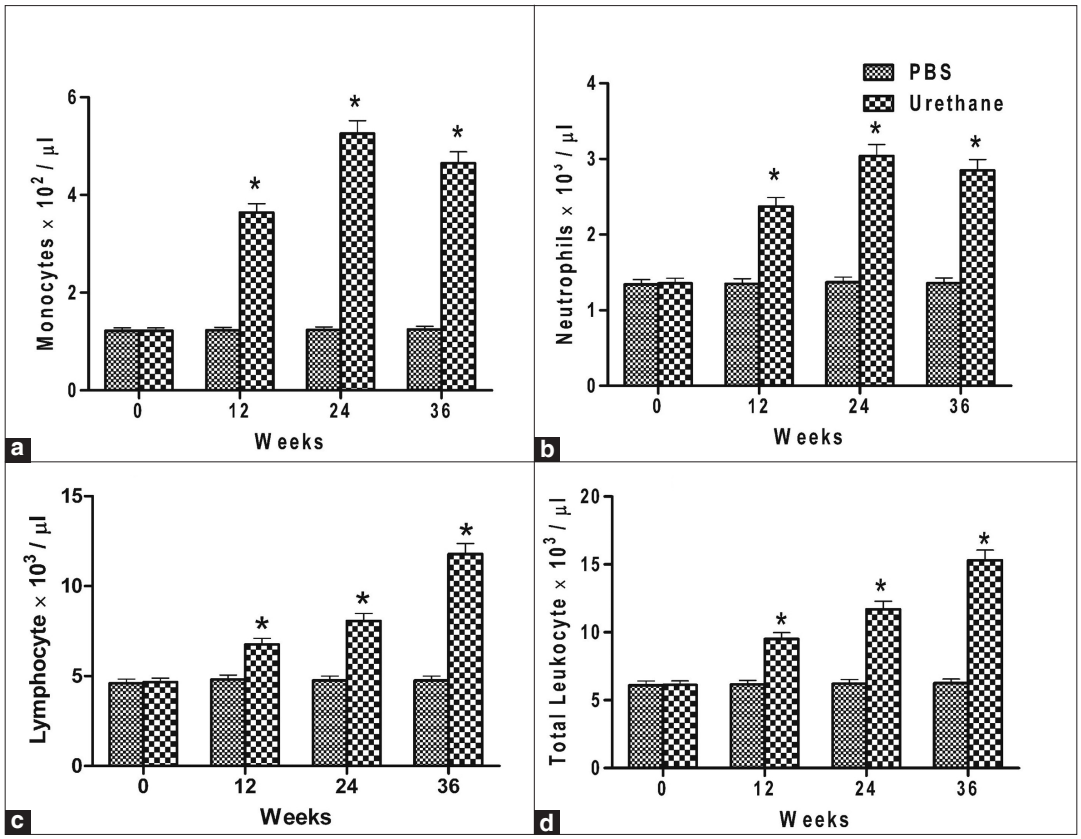


**Figure 4: The numbers of circulatory inflammatory cells in the PBS-injected and urethane-injected mice blood (a) monocytes, (b) neutrophils, (c) lymphocytes, and (d) leukocytes. Increases in the numbers of cells were found in urethane-injected mice in comparison to PBS-injected control mice. (Data reported as the mean ± SEM for n = 8 per group and compared against PBS-injected mice by using a Student t-test. *P* < 0.05 were considered significant.)**

the serum of urethane-injected mice as compared to PBS-injected mice [Figure 7a]. The level of IL-6 protein was also found elevated by 1.3, 1.97, and 2.43 folds at 12, 24, and 36 week, respectively, in the serum of urethane-injected mice as compared to PBS-injected mice [Figure 7a]. The level of IL-1β and IL-6 increased with time in urethane-injected mice serum samples, while in the PBS-injected mice serum samples the levels of both cytokines were approximately constant along with time [Figure 7].

### EMSA of NF-κB and Stat3

To show the urethane-mediated activation and binding of TF, NF-κB, and Stat3 present in the urethane-injected lung tissues of mice, NF-κB and Stat3 specific biotin-labeled oligonucleotide consensus sequence was used to perform EMSA. Results suggest shift in the consensus oligonucleotide sequence of NF-κB [Figure 8; Lane 1] and Stat3 [Figure 9; Lane 1] after comparatively more binding of TF, NF-κB, and Stat3 of nuclear extract of urethane primed lung tissues in comparison to PBS primed nuclear extract [Figure 8; Lane 2 and Figure 9; Lane 2], respectively, in NF-κB and Stat3. Lane 3 of Figures 8 and 9 show NF-κB and Stat3 specific biotin-labeled oligonucleotide consensus sequence without nuclear extract, respectively.

## DISCUSSION

In the present study, our motivation was to understand the possible mechanism and cause of lung tumor development after i.p. injection of urethane in Balb/c mice model. We report here that the urethane-induced lung tumor genesis in Balb/c mice is due to chronic inflammation occurred in the lung. The chronic inflammation is due to increase in the expression of pro-inflammatory cytokines (IL-1β and IL-6), activation and expression of NF-κB [Figure 8] and Stat3 [Figure 9] in the urethane-injected mice lung tissues. Upregulated expression might have subsequently created microenvironment to play a pivotal role in the urethane-induced lung tumor formation.

After tumor development, the average body weight of urethane-injected mice decreased in comparison to PBS-injected mice [Figure 1], whereas the lung organ index of urethane-injected mice increased as compared to lung organ index of PBS-injected mice [Figure 2]. This increase in the lung organ index of urethane-injected mice is due to

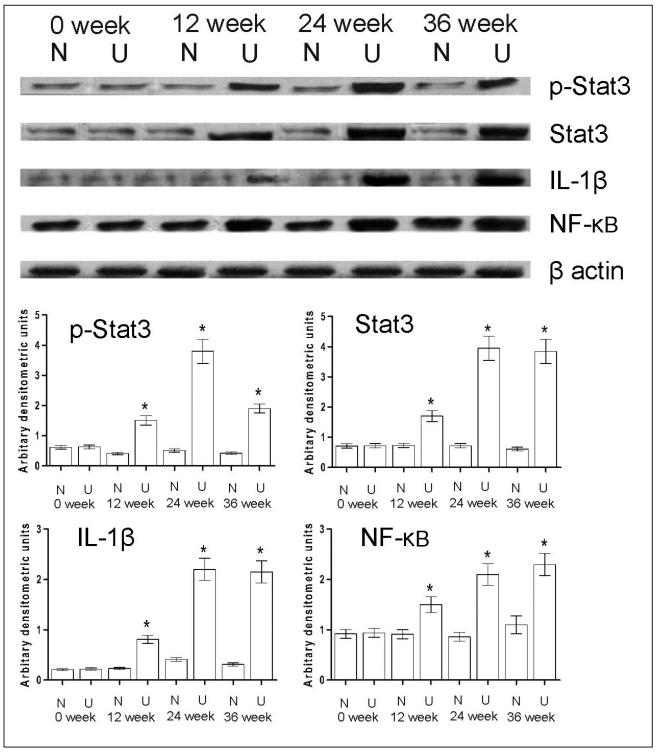


**Figure 5: Western blot showing expression level of pStat3, Stat3, NF-κB, and IL-β protein samples of lung tissues of urethane-injected mice (U) and PBS-injected control mice (N) at 0, 12, 24, and 36 weeks. β-actin was used as loading control. Densitometry was performed to generate graph**

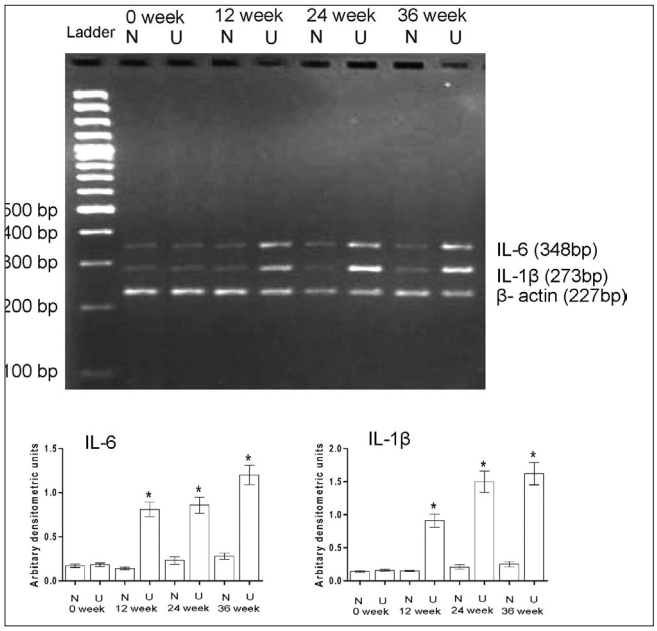


**Figure 6: RT-PCR showing the expression level of proinflammatory cytokines interleukin-6 and interleukin-1β at transcriptional level in lung tissues of urethane-injected mice (U) and PBS-injected control mice (N) at 0, 12, 24, and 36 weeks. β-actin was used to show that equal amount of cDNA was used for PCR. Densitometry was performed after normalization with β-actin to generate graph**

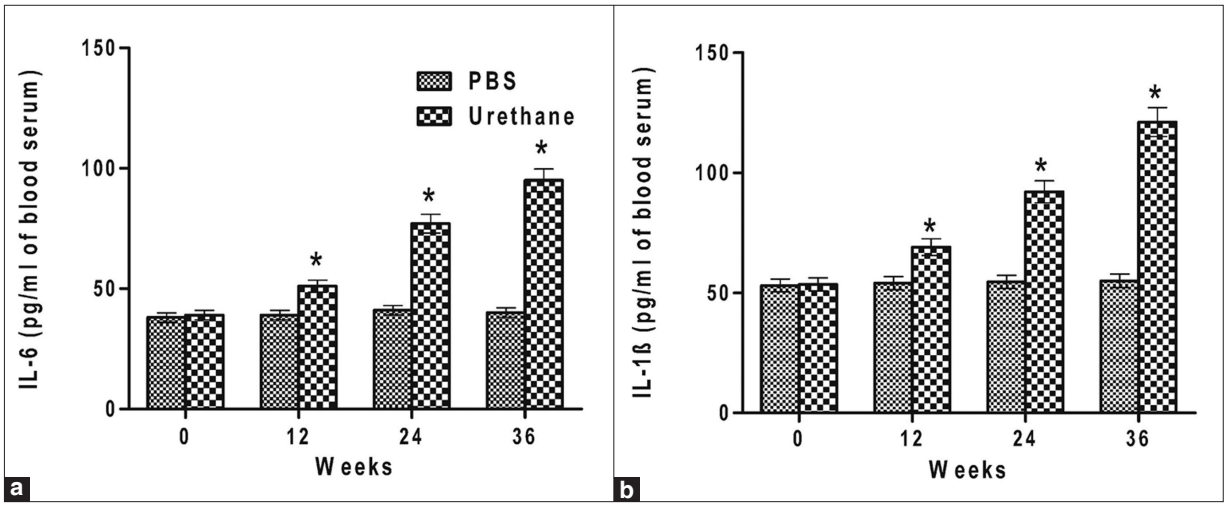


**Figure 7: The level of IL-1β (a) and IL-6 (b) in serum was measured by ELISA in urethane-injected mice and PBS-injected mice. (Data reported as the mean ± SEM for n = 8 per group and compared against PBS-injected by using a Student t-test. *P* < 0.05 were considered significant.)**

increase in the size and weight of lungs and overall decrease in the body weight after tumor genesis and development. The step-wise development of tumors were also observed in urethane-injected lung tissues of mice [Figures 3b–3d]. AAH is a precursor lesion of AD as we observed in our result [Figure 3], which is in accordance with earlier reported.[20]

The multiple doses of i.p. injection of urethane in mice increased the population of circulating inflammatory cells (monocytes, neutrophils, and lymphocytes) in peripheral blood [Figure 4]. All inflammatory cells latter suppose to get recruited at the site of lung tissues damage [21] and secrete large amount of inflammatory cytokines and chemokines to promote the outgrowth of neoplastic cells to trigger

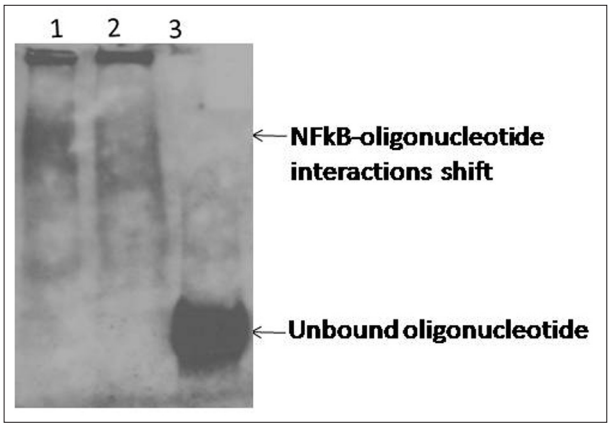


**Figure 8: EMSA shows activation and binding of NF-κB to its biotin-labeled oligonuleotide consensus sequence. Lane 1, urethane-injected mice lung tissue nuclear extract showing NF-κB binding with consensus oligonucleotide NF-κB binding sequence and shift; Lane 2, PBS (phosphate buffer saline) injected mice lung tissue nuclear extract showing Stat3 binding with consensus oligonucleotide NF-κB binding sequence and shift; Lane3, only consensus oligonucleotide NF-κB binding sequence**

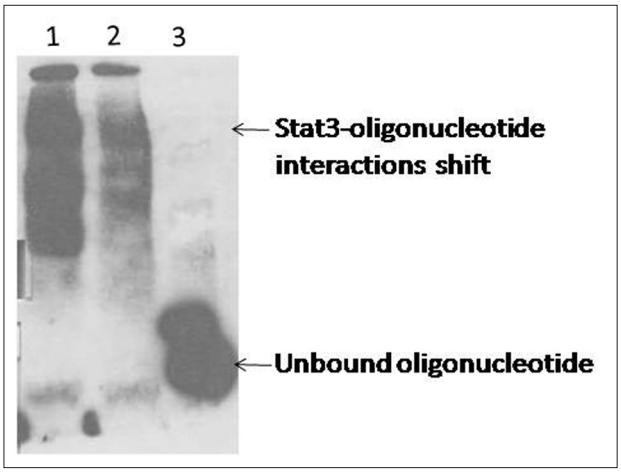


**Figure 9: EMSA shows activation and binding of Stat3 to its biotin-labeled oligonuleotide consensus sequence. Lane 1, Urethane-injected mice lung tissue nuclear extract showing Stat3 binding with consensus oligonucleotide Stat3 binding sequence and shift; Lane 2, PBS (phosphate buffer saline) injected mice lung tissue nuclear extract showing Stat3 binding with consensus oligonucleotide Stat3 binding sequence and shift; Lane3, only consensus oligonucleotide Stat3 binding sequence**

probably persistent inflammation. At transcriptional level, we observed upregulated expression of pro-inflammatory cytokines IL-1β and IL-6 in urethane-injected mice lung tissues as compared to PBS-injected mice lung tissues, as shown in Figure 6, which is similar to the observation of other researcher in the gastric cancer tissues.[22] The significant upregulated expression level of these cytokines up to 24 week and thereafter the expression level become almost constant in urethane-injected lung tissues but not in the PBS-injected mice lung tissues suggests that urethane persistently upregulates the expression level of pro-inflammatory cytokines which have created microenvironment for the activation of possible signaling pathways for lung carcinogenesis. This fact is well supported by the earlier reports that IL-1β and IL-6 activates the NF-κB and Stat3.[23-26] The upregulated expression of TF such as NF-κB, Stat3, and pStat3 in the urethane-injected lung tissues [Figure 5], which is up to 24 week and there after saturation in the expression level was observed up to 36 week in urethane-injected lung tissues. Shows the constitutive expression of these TF such constitutive expression might be essential requirement for tumor genesis and progression. In contrast, we observed significantly lower but equal expression level of above TF in PBS-injected mice lung tissue [Figure 5], where tumor genesis was absent.

However, these results suggest that urethane is responsible for the upregulation, activation, and expression of NF-κB and Stat3 via pro-inflammatory cytokines IL-1β and IL-6 which is well supported by earlier reports that cytokines modulate the expression of genes involved in cell-cycle progression and inhibition of apoptosis via the NF-κB and Stat3 pathways.[27-29] The NF-κB and Stat3 both TF have been identified as an important promoter of tumorgenesis (AD) in oral keratinocytes and gastrointestinal tract[30,31] as we also observed in the case of mice lung adenocarinoma. TF, NF-κB, and Stat3 are key molecules to regulate the genes responsible for the production of pro-inflammatory cytokines and chemokines.[32,33] Probably activated NF-κB [Figure 8] and Stat3 [Figure 9] bind separately or in cooperate to each other within promoter region of many target genes[23,34,35] to promote constitutive expression of cytokines, inflammatory cells proliferation, metastasis and angiogenesis, as well as protect tumor cells from apoptosis by regulating associated cancerous genes.[36-38] Moreover, several other target genes responsible for chronic inflammation[39] might got upregulated by the both TF. Our ELISA results suggested the enhanced production and secretion of pro-inflammatory cytokines in urethane-injected mice serum than those in PBS-injected mice serum, indicate the role of tumor cells and infected pro-inflammatory cells in creating chronic inflammatory microenvironment by secreting IL-1β & IL-6 to enhance cell proliferation and uninterrupted growth of alveolar epithelial cells leading to tumor genesis and development in the urethane-induced Balb/c mice lung.

Moreover, TF NF-κB and Stat3 seem to create a potential molecular bridge between IL-β and IL-6 mediated inflammation and lung tumor development in urethane-injected mice. Our results support the above hypothesis that pro-inflammatory IL-β and IL-6 cytokines initially secreted by circulatory inflammatory cells might have

upregulated the expression and activation of NF-κB and Stat3. Consequently, the constitutive expression of NF-κB and Stat3 promoted the transcription of pro-inflammatory cytokine genes in tumor cells [Figure 6] and tumor-associated stromal cells creating a sustained chronic inflammatory state within the tumor-microenvironment.[40]

In conclusion, urethane-induced lung tumor generation in Balb/c mice model enable us to understand the mechanisms involved in the genesis and development of tumor in the lungs along with the molecules or factors involved in the cancer progression. The upregulation of potential inflammatory cytokines IL-1β and IL-6 followed by the activation and upregulation of TF, NF-κB, and Stat3 lead to chronic inflammation, subsequently the upregulation of cancerous genes to make the lung cells cancerous leading to lung's tumor formation.

## ACKNOWLEDGMENTS

Chandradeo Narayan is thankful to UGC-CSIR for granting junior research fellowships to carry on this research work. We render our sincere thanks to Mr. Sunil Kr. Yadav for taking care of experimental animals.

## REFERENCES

1. Jemal A, Siegel R, Ward E, Hao Y, Xu J, Thun MJ. Cancer statistics 2009. CA Cancer J Clin 2009;59:225-49.
2. Youlden DR, Cramb SM, Baade PD. The International Epidemiology of Lung Cancer: geographical distribution and secular trends. J Thorac Oncol 2008;3:819-31.
3. Minna JD, Roth JA, Gazadar AF. Focus on lung cancer. Cancer Cell 2002;1:49-52.
4. Schmid K, Angestein N, Geleff S, Gschwandtner A. Quantitative texture features analysis confirms WHO classification 2004 for lung carcinomas. Mod Pathol 2006;19:453-9.
5. Gazdar AF, Linnoila RI. The pathology of lung cancer--changing concepts and newer diagnostic techniques. Semin Oncol 1988;15: 215-25.
6. Philip M, Rowley DA, Schreiber H. Inflammation as a tumor promoter in cancer induction. Semin Cancer Biol 2004;14:433-9.
7. Surh YJ, Chun K, Cha HH, Han SS, Keum YS, Park KK, *et al*. Molecular mechanism underlying chemopreventive activities of ant-inflammatory phytochemicals: down-regulation of COX-2 and iNOS through suppression of NF-κB activation. Mutat Res 2001;480-481:243-68.
8. Schmetiz I, Chiong KG, Hoffmann DJ. Formation and dtermination of ethyl carbamate in tobacco and tobacco smoke. Anal Toxicol 1978;2:265-8.
9. Ough CS. Ethylcarbamate in fermented beverages and foods. I. Naturally occurring ethylcarbamate. J Agric Food Chem 1976;24:323-8.
10. Delledonne D, Rivetti F, Romano U. Development in the production and application of dimethylcarbonate. Applied catalysis A: General 2001;221:241-51.
11. Wang D, Yang B, Zhai X, Zhou L. Synthesis of diethyl carbonate by catalytic alcoholysis of urea. Fuel Processing Technol 2007;88:807-12.
12. Hasnip S, Crews C, Potter N, Christy J, Chan D, Bondu T, *et al*. Survey of ethyl carbamate in fermented foods sold in the United Kingdom in 2004. J Agric Food Chem 2007;55:2755-9.
13. Alexander J, Auounsson GA, Benford D, Cockburn A, Cravedi J, Doglitti E, *et al*. Ethyl carbamate and hydrocyanic acid in food and beverages. Scientific opinion of the panel on contaminants. EFSA Journal 2007;551:1-44.
14. Park SK, Kim CT, Lee JW, Jhee OH, Om AS, Kang JS, *et al*. Analysis of ethyl carbamate in Korean soy sauce using high-performance liquid chromatography with fluorescence detection or tandem mass spectrometry and gas spectrometry with mass spectrometry. Food Control 2007;18:975-82.
15. Malkinson AM. Molecular comparison of human and mouse pulmonary adenocarcinomas. Exp Lung Res 1998;24:541-55.
16. Malikinson AM. Primary lung tumors in mice as an aid for understanding, preventing, and treating human adenocarcinoma of the lung. Lung Cancer 2001;32:265-79.
17. Malkinson AM, Beer DS. Major effect on susceptibility to urethan-induced pulmonary adenoma by a single gene in BALB/cBy mice. J Natl Cancer Inst 1983;70:931-6.
18. Malkinson AM. Primary lung tumors in mice: an experimentally manipulable model of human adenocarcinoma. Cancer Res 1992;52(9 Suppl):2670s-76s.
19. Manson RJ, Kalina M, Nielson LD, Malkinson AM, Shannon JM. Surfactant protein C expression in urethane-induced murine pulmonary tumors. Am J Pathol 2000;156:175-82.
20. Mori M, Rao SK, Popper HH, Cagle PT, Fraire AE. Atypical adenomatous hyperplasia of the lung: a probable forerunner in the development of adenocarcinoma of the lung. Mod Pathol 2001;14:72-84.
21. Redente EF, Orliky DJ, Bouchard RJ, Malkinson AM. Tumor signaling to the bone marrow changes the phenotype of monocytes and pulmonary macrophages during urethane-induced primary lung tumorigenesis in A/J mice. Am J Pathol 2007;170:693-708.
22. Kai H, Kitadai Y, Kodama M, Cho S, Kurodo T, Ito M, *et al*. Involvement of pro-inflamatory cytokines IL-1β and IL-6 in progression of human gastric carcinoma. Anticancer Res 2005;25:709-13.
23. Yoshida Y, Kumar A, Koyama Y, Peng H, Arman A, Boch JA, *et al*. IL-1 activates STAT3/NFkB cross-talk via unique TRAF6 and p65 dependent mechanism. J Biol Chem 2004;279:1768-76.
24. Vane JR, Bakhle YS, Botting RM. Cycloooxygenases 1 and 2. Annu Rev Pharmacol Toxicol 1998;38:97-120.
25. Neurath MF, Becker C, Barbulescu K. Role of NF-kappaB in immune and inflammatory responses in the gut. Gut 1998;43:856-60.
26. Zhong Z, Wen Z, Darnell JE Jr. Stat3: a SATA family member activated by tyrosine phosphorylation in response to epidermal growth factor and interleukin-6. Science 1994;264:95-8.
27. Yoshimura A. Signal transduction of inflammatory cytokines and tumor development. Cancer Sci 2006;97:439-47.
28. Rose-John S, Schooltink H. Cytokines are a therapeutic target for the prevention of inflammation-induced cancers. Recent Results Cancer Res 2007;174:57-66.
29. Voronov E, Carmi Y, Apte RN. Role of IL-1-mediated inflammation in tumor angiogenesis. Adv Exp Med Biol 2007;601:265-70.
30. Arredono J, Chernyavsky AI, Jolkovsky DL, Pinkerton KE, Grando SA. Receptor-mediated tobacco toxicity: cooperation of the Ras/Raf-1/MEK1/ERK and JAK-2/STAT-3 pathways downstream of alpha7 nicotinic receptor in oral keratinocytes. FASEB J 2006;20:2093-101.
31. Greten FR, Eckmann L, Greten TF, Park JM, Li ZW, Egan LJ, *et al*. Ικκ beta links inflammation and tumorigenesis in a mouse model of colitis associated cancer. Cell 2004;118:285-96.
32. Aggarawal BB, Kunnumakkara AB, Harikumar KB, Gupta SR, Tharakan ST, Koca C, *et al*. Signal transducer and activator of transcription-3, inflammation, and cancer: how intimate is the relationship? Ann N Y Acad Sci 2009;1171:59-76.
33. Karin M, Yamamoto Y, Wang QM. The Ικκ NF-kappa B: system a treasure trove for drug development. Nat Rev Drug Discov 2004;3:17-26.
34. Darnell JE Jr . STATs and gene regulation. Science 1997;277:1630-5.
35. Perkins ND. NF-kappaB: tumor promoter or suppressor? Trends Cell Biol 2004;14:64-9.
36. Huang S. Regulation of metastases by signal transducer and activator of transcription 3 signaling pathway: clinical implications. Clin Cancer Res 2007;13:1362-6.
37. Niu G, Wright KL, Huang M, Song L, Haura E, Turkson J, *et al*. Constitutive Stat3 activity up-regulates VEGF expression and tumor angiogenesis. Oncogene 2002;21:2000-8.
38. Xie TX, Wei D, Liu M, Gao AC, Ali-Osman F, Sawaya R, *et al*. Stat3 activation regulates the expression of matrix metalloproteinase-2 and tumor invasion

and metastasis. Oncogene 2004;23:3550-60.
39. Chen F, Castranova V, Shi X. New insights into the role of nuclear factor-κB in cell growth regulation. Am J Pathol 2001;159:387-97.
40. Lu H, Ouyang W, Huang C. Inflammation, a key event in cancer development. Mol Cancer Res 2006;4:221-33.

**How to cite this article:** Narayan C, Kumar A. Constitutive over expression of IL-1β, IL-6, NF-κB, and Stat3 is a potential cause of lung tumorgenesis in urethane (ethyl carbamate) induced Balb/c mice. J Carcinog 2012;11:9.

**Source and Support:** Nil. **Conflict of Interest:** None declared.

## AUTHOR'S PROFILE

**Mr. Chandradeo Narayan,** School of Biotechnology, Faculty of Science, Banaras Hindu University, Varanasi, India

**Dr. Arvind Kumar (Ph.D.),** School of Biotechnology, Faculty of Science, Banaras Hindu University, Varanasi